24th COBEM - 2017

24th ABCM International Congress of Mechanical Engineering
December 3-8, 2017, Curitiba, PR, Brazil

COBEM-2017-1054
MODELING OF A 4-DOF CONTROL MOMENT GYROSCOPE

Fabio Yukio Toriumi
Bruno Augusto Angélico
Escola Politécnica da USP – Departamento de Engenharia de Telecomunicações e Controle
Av. Prof. Luciano Gualberto 158, travessa 3, CEP 05508-900, São Paulo, SP, Brazil
fabioyt@usp.br
angelico@lac.usp.br

Roberto Spinola Barbosa
Flavius Portella Ribas Martins
Escola Politécnica da USP – Departamento de Engenharia Mecânica
Av. Prof. Mello Moraes 2231, CEP 05508-030, São Paulo, SP, Brazil
roberto.barbosa@poli.usp.br
flavius.martins@poli.usp.br

Tarcisio Antonio Hess Coelho
Escola Politécnica da USP – Departamento de Engenharia Mecatrônica e de Sistemas Mecânicos
Av. Prof. Mello Moraes 2231, CEP 05508-030, São Paulo, SP, Brazil
tarcisio.coelho@poli.usp.br

Abstract. *Control moment gyroscopes (CMGs) are used as actuators in some applications like satellites and spacecrafts attitude control, and stabilization. A good system model is fundamental for control applications. This paper presents a detailed modeling process of a four degrees of freedom (DOF) CMG unit, which kinematics stage is based on a defined convention using quaternion algebra, and dynamics stage is based on Gibbs-Appell equations in Kane's proposed dynamical equations form. Two tests that analyze the main characteristics of the plant are considered in order to validate the generated nonlinear model, which numerical simulations results are compared to the practical experiments.*

Keywords: *Control Moment Gyroscope, Multibody Systems, System Modeling, Quaternions, Gibbs-Appell.*

1. INTRODUCTION

Control moment gyroscopes (CMGs) are used as torque actuators in some applications like satellites and spacecrafts attitude control (Yavuzoglu *et al.*, 2011; Bhat and Tiwari, 2009), and for stabilization (Gagne *et al.*, 2012; Yetkin *et al.*, 2014). This kind of gyroscope is generally composed of a spinning rotor and two or more motorized gimbals that change the rotor angular momentum direction, generating a reaction called "gyroscopic torque".

An example unit of CMG is the model 750 from Educational Control Products (ECP) manufacturer. This electromechanical plant has an axisymmetric brass disc suspended in an assembly with four angular degrees of freedom (DOF). Many papers proposed several approaches for its attitude control (Abbas *et al.*, 2013, 2014; Mardan *et al.*, 2015; Durand *et al.*, 2014), all based on linearized model obtained from the ECP manual (Parks, 1999), which does not describe the modeling process.

In this paper, the modeling of model 750 CMG from ECP is proposed, which kinematics stage is based on defined convention in Craig (1989) using quaternion algebra (Kuipers, 1999), and dynamics stage is based on Gibbs-Appell equations in Kane's proposed dynamical equations form (Kane *et al.*, 1983; Baruh, 1999). The bearings friction of plant joints are not considered in modeling process.

The proposition to use quaternion algebra in kinematics stage aim a future work on full quaternion based modeling, in which quaternion algebra is used in both kinematics and dynamics stages.

Two tests to analyze the plant main characteristics (precession and nutation) were considered in order to validate the generated plant nonlinear model, which numerical simulations results are compared to the practical experiments.

2. CMG MODELING

2.1 Plant description

Figure 1 illustrates and describes ECP model 750 CMG unit, which is comprised of four rigid bodies (bodies A, B, C, and D), which angular positions θ_k ($k = 1, 2, 3, 4$) are respectively measured by incremental encoders A, B, C, and D, and two DC motors (motors $\#1$ and $\#2$). Motor $\#1$ rotates body D (the axisymmetric brass disc, called rotor) around axis $\#4$ and motor $\#2$ rotates body C (the inner gimbal) around axis $\#3$. Bodies A (the rotating base) and B (the outer gimbal) do not have active applied torques and rotate only by plant reactions. Each one of these two bodies has a brake installed on its rotation axes (axes $\#1$ and $\#2$, respectively), that can be actuated via a toggle switch to lock their angular positions θ_1 and θ_2 and hence reduce the system DOF.

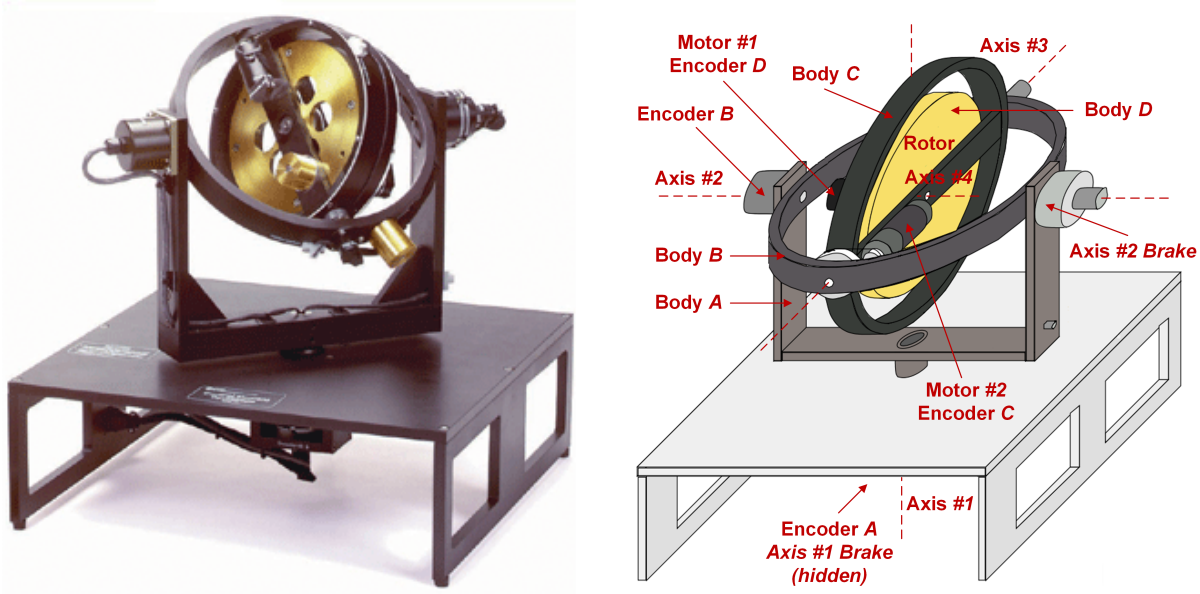

(a) Plant illustration (ECP, 1990)

(b) Plant description

Figure 1: Illustration and description of ECP model 750 CMG unit.

Considering the brakes deactivated, when the rotor angular velocity varies, body B rotates around axis $\#2$ in the opposite direction by reaction, obeying the conservation principle of angular momentum, and when the inner gimbal is tilted while rotor is rotating, body A is rotated around axis $\#1$ by the generated gyroscopic torque.

As the plant has incremental encoders, they need to be set to zero at the beginning of every test procedure. Figure 1b reflects $\theta_k = 0$ radians ($k = 1, 2, 3, 4$), in which:

- θ_1 can be set to zero at any position of body A, since all CMG bodies are assumed to be symmetric;
- θ_2 is set to zero with body B oriented perpendicular to body A;
- θ_3 is set to zero with body C oriented perpendicular to body B; and
- θ_4 can be set to zero at any position of body D, since it is axisymmetric.

2.2 Kinematics stage

Before initiate the modeling process, it is necessary to attach a frame to each CMG body in order to describe its relative orientation. So, this paper applies the convention defined in Craig (1989), in which frames $\{i\}$, composed of dextral sets of orthogonal unit vectors $\widehat{x}_i$, $\widehat{y}_i$ and $\widehat{z}_i$, are attached rigidly to all bodies. Figure 2 illustrates the resulting CMG bodies attached frames $\{k\}$ ($k = 1, 2, 3, 4$), the inertial reference frame $\{0\}$ attached to the CMG fixed base, and motors $\#1$ and $\#2$ applied torques T_1 and T_2, respectively. All these frames have its origins fixed located at rotor center (since all CMG bodies are assumed to be symmetric), although they are dislocated in Fig. 2 for better visualization.

In kinematics stage, the 3×1 bodies angular velocity vectors ${}^{k}\boldsymbol{\omega_k}$ are calculated, given by the following iterative formulation (Craig, 1989):

$$ {}^{k}\boldsymbol{\omega_k} = {}^{k}_{k-1}\boldsymbol{R} \cdot {}^{k-1}\boldsymbol{\omega_{k-1}} + \begin{bmatrix} 0 & 0 & \dot{\theta}_k \end{bmatrix}^{\mathsf{T}}, \quad (k = 1, 2, 3, 4), \tag{1} $$

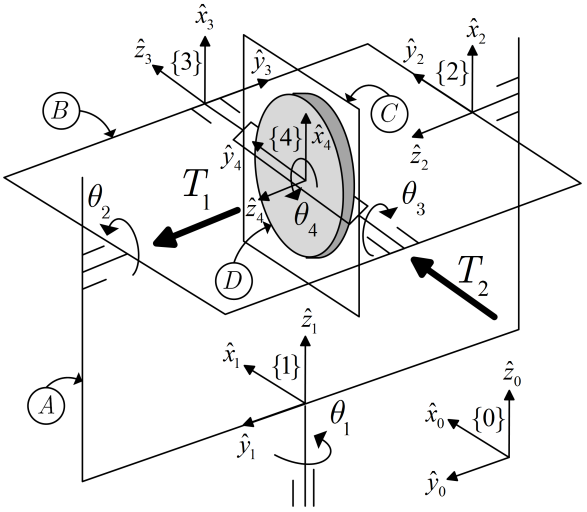

Figure 2: Resulting bodies attached frames.

composed of bodies angular velocities $\dot{\theta}_k$ in $\widehat{z}_k$ direction and 3×3 rotation matrices $\mathbf{^{k}_{k-1}R}$ with direction cosines elements:

$$\mathbf{^{1}_{0}R}=\begin{bmatrix} c_{\theta_1} & s_{\theta_1} & 0 \\ -s_{\theta_1} & c_{\theta_1} & 0 \\ 0 & 0 & 1 \end{bmatrix},\ \mathbf{^{2}_{1}R}=\begin{bmatrix} s_{\theta_2} & 0 & c_{\theta_2} \\ c_{\theta_2} & 0 & -s_{\theta_2} \\ 0 & 1 & 0 \end{bmatrix},\ \mathbf{^{3}_{2}R}=\begin{bmatrix} c_{\theta_3} & 0 & -s_{\theta_3} \\ -s_{\theta_3} & 0 & -c_{\theta_3} \\ 0 & 1 & 0 \end{bmatrix} \text{ and } \mathbf{^{4}_{3}R}=\begin{bmatrix} c_{\theta_4} & 0 & s_{\theta_4} \\ -s_{\theta_4} & 0 & c_{\theta_4} \\ 0 & -1 & 0 \end{bmatrix}, \quad (2)$$

where $c_{\theta_k}=\cos(\theta_k)$ and $s_{\theta_k}=\sin(\theta_k)$ $(k=1,2,3,4)$.

These rotation matrices $\mathbf{^{k}_{k-1}R}$ describe the orientation of frame $\{k-1\}$ relative to $\{k\}$ and use the algebra of matrix rotation operator. At this point, the quaternion algebra (Kuipers, 1999) will be considered, whose rotation operator have some algebraic relationships with the matrix one. Some of these relationships are exposed here and others can be searched at Jazar (2010); Dam *et al.* (1998); Spring (1986); Funda *et al.* (1990).

A quaternion $\boldsymbol{q}$ is a hyper-complex number of rank four, which may be regarded as a four-tuple of real numbers (i.e. as an element of $\mathcal{R}^4$, which orthonormal basis is given by four unit vectors $\widehat{r}=(1,0,0,0)$, $\widehat{x}=(0,1,0,0)$, $\widehat{y}=(0,0,1,0)$ and $\widehat{z}=(0,0,0,1)$), represented as $\boldsymbol{q}=(q_0,q_1,q_2,q_3)$, where q_n $(n=0,1,2,3)$ are called the components of the quaternion, which are simply real numbers or scalars (Kuipers, 1999). It can also be represented in an alternative way, defining q_0 as its scalar part and its vector part $\vec{\boldsymbol{q}}$ as an ordinary vector in $\mathcal{R}^3$, given by $\vec{\boldsymbol{q}}=\widehat{x}q_1+\widehat{y}q_2+\widehat{z}q_3$, where the three unit vectors $\widehat{x}=(1,0,0)$, $\widehat{y}=(0,1,0)$ and $\widehat{z}=(0,0,1)$ form the orthonormal basis for $\mathcal{R}^3$. It is adopted to consider this last representation in your vector form, as well as its complex conjugate $\boldsymbol{q}^*$:

$$\boldsymbol{q}=q_0+\vec{\boldsymbol{q}}=q_0+\widehat{x}q_1+\widehat{y}q_2+\widehat{z}q_3=\begin{bmatrix} q_0 & q_1 & q_2 & q_3 \end{bmatrix}^{\mathsf{T}} \text{ and } \boldsymbol{q}^*=q_0-\vec{\boldsymbol{q}}=\begin{bmatrix} q_0 & -q_1 & -q_2 & -q_3 \end{bmatrix}^{\mathsf{T}}. \quad (3)$$

In quaternions algebra, the set of quaternions under the operation of addition satisfy all of the axioms of a field, i.e. considering two quaternions $\boldsymbol{q}=q_0+\vec{\boldsymbol{q}}$ and $\boldsymbol{p}=p_0+\vec{\boldsymbol{p}}$, they are equal if and only if they have exactly the same components $(q_n=p_n,\, n=0,1,2,3)$ and their sum is defined by adding their correspondent components:

$$\boldsymbol{q}+\boldsymbol{p}=(q_0+p_0)+\widehat{x}(q_1+p_1)+\widehat{y}(q_2+p_2)+\widehat{z}(q_3+p_3)=\begin{bmatrix} q_0+p_0 & q_1+p_1 & q_2+p_2 & q_3+p_3 \end{bmatrix}^{\mathsf{T}}. \quad (4)$$

And under the operation of multiplication, the set of quaternions satisfy all of the axioms of a field except for the commutative law, i.e. considering a scalar α and the quaternion $\boldsymbol{q}$, their product is given by:

$$\alpha\boldsymbol{q}=\alpha q_0+\alpha\vec{\boldsymbol{q}}=\alpha q_0+\widehat{x}\alpha q_1+\widehat{y}\alpha q_2+\widehat{z}\alpha q_3=\begin{bmatrix} \alpha q_0 & \alpha q_1 & \alpha q_2 & \alpha q_3 \end{bmatrix}^{\mathsf{T}}, \quad (5)$$

and the product of two quaternions is defined so that to satisfy the special products:

$$\widehat{x}^2=\widehat{y}^2=\widehat{z}^2=\widehat{x}\widehat{y}\widehat{z}=-1,\ \widehat{x}\widehat{y}=\widehat{z}=-\widehat{y}\widehat{x},\ \widehat{y}\widehat{z}=\widehat{x}=-\widehat{z}\widehat{y} \text{ and } \widehat{z}\widehat{x}=\widehat{y}=-\widehat{x}\widehat{z}, \quad (6)$$

which are not commutative. Thereby, the quaternion product of $\boldsymbol{q}$ and $\boldsymbol{p}$, denoted as $\boldsymbol{q}\otimes\boldsymbol{p}$, is given by:

$$\boldsymbol{q}\otimes\boldsymbol{p}=(q_0+\vec{\boldsymbol{q}})(p_0+\vec{\boldsymbol{p}})=(q_0+\widehat{x}q_1+\widehat{y}q_2+\widehat{z}q_3)(p_0+\widehat{x}p_1+\widehat{y}p_2+\widehat{z}p_3)=\begin{bmatrix} q_0p_0-q_1p_1-q_2p_2-q_3p_3 \\ q_0p_1+q_1p_0+q_2p_3-q_3p_2 \\ q_0p_2-q_1p_3+q_2p_0+q_3p_1 \\ q_0p_3+q_1p_2-q_2p_1+q_3p_0 \end{bmatrix}, \quad (7)$$

which is different from $\boldsymbol{p} \otimes \boldsymbol{q}$:

$$\boldsymbol{p} \otimes \boldsymbol{q} = (p_0 + \vec{\boldsymbol{p}})(q_0 + \vec{\boldsymbol{q}}) = (p_0 + \widehat{x}p_1 + \widehat{y}p_2 + \widehat{z}p_3)(q_0 + \widehat{x}q_1 + \widehat{y}q_2 + \widehat{z}q_3) = \begin{bmatrix} p_0q_0 - p_1q_1 - p_2q_2 - p_3q_3 \\ p_0q_1 + p_1q_0 + p_2q_3 - p_3q_2 \\ p_0q_2 - p_1q_3 + p_2q_0 + p_3q_1 \\ p_0q_3 + p_1q_2 - p_2q_1 + p_3q_0 \end{bmatrix}. \quad (8)$$

Another important algebraic concept relating to quaternions is its norm, a scalar denoted by $|\boldsymbol{q}|$, defined by $|\boldsymbol{q}| = \sqrt{\boldsymbol{q}^* \otimes \boldsymbol{q}} = \sqrt{q_0^2 + q_1^2 + q_2^2 + q_3^2}$. If a quaternion has norm equal to 1, then it is called a unit quaternion, which components q_n ($n = 0, 1, 2, 3$) have absolute values less than or equal to 1. Consequently, as the inverse of a quaternion $\boldsymbol{q}$ is given by $\boldsymbol{q}^{-1} = \boldsymbol{q}^*/|\boldsymbol{q}|^2$, the inverse of a unit quaternion is simply its complex conjugate ($\boldsymbol{q}^{-1} = \boldsymbol{q}^*$) (Jazar, 2010).

Knowing all these basic operations in quaternion algebra, it is possible to list one of the algebraic relationships between its rotation operator with the matrix one:

$$\underbrace{{}^{\boldsymbol{k}}_{\boldsymbol{k-1}}\boldsymbol{R} \cdot {}^{\boldsymbol{k-1}}\boldsymbol{\omega_{k-1}}}_{\text{Matrix rotation operator}} \Rightarrow \underbrace{{}^{\boldsymbol{k}}_{\boldsymbol{k-1}}\boldsymbol{q} \otimes {}^{\boldsymbol{k-1}}\overline{\boldsymbol{\omega}}_{\boldsymbol{k-1}} \otimes {}^{\boldsymbol{k}}_{\boldsymbol{k-1}}\boldsymbol{q}^*}_{\text{Quaternion rotation operator}}, \quad (k = 1, 2, 3, 4). \quad (9)$$

The matrix rotation operator is composed of rotation matrices ${}^{\boldsymbol{k}}_{\boldsymbol{k-1}}\boldsymbol{R}$, defined in Eq. (2), that act on angular velocity vectors ${}^{\boldsymbol{k-1}}\boldsymbol{\omega_{k-1}}$. And the quaternion rotation operator is composed of unit quaternions ${}^{\boldsymbol{k}}_{\boldsymbol{k-1}}\boldsymbol{q}$ and ${}^{\boldsymbol{k}}_{\boldsymbol{k-1}}\boldsymbol{q}^*$, which the last one is the complex conjugate of the first, and the equivalent angular velocity vectors in quaternion form ${}^{\boldsymbol{k-1}}\overline{\boldsymbol{\omega}}_{\boldsymbol{k-1}} = \begin{bmatrix} 0 & {}^{\boldsymbol{k-1}}\boldsymbol{\omega_{k-1}} \end{bmatrix}^\intercal$, which is called a pure quaternion since its scalar part is null.

The equivalent rotation matrix ${}^{\boldsymbol{k}}_{\boldsymbol{k-1}}\boldsymbol{R}$ in quaternion form ${}^{\boldsymbol{k}}_{\boldsymbol{k-1}}\boldsymbol{q}$ is given by (Craig, 1989):

$${}^{\boldsymbol{k}}_{\boldsymbol{k-1}}\boldsymbol{R} = \begin{bmatrix} r_{11} & r_{12} & r_{13} \\ r_{21} & r_{22} & r_{23} \\ r_{31} & r_{32} & r_{33} \end{bmatrix} \Rightarrow {}^{\boldsymbol{k}}_{\boldsymbol{k-1}}\boldsymbol{q} = \frac{1}{2\sqrt{\delta}} \begin{bmatrix} \delta \\ r_{32} - r_{23} \\ r_{13} - r_{31} \\ r_{21} - r_{12} \end{bmatrix}, \text{ where } \delta = r_{11} + r_{22} + r_{33} + 1, \quad (10)$$

and calculating the quaternion equivalent form of rotation matrices in Eq. (2), results in the following rotation quaternions:

$${}^{\boldsymbol{1}}_{\boldsymbol{0}}\boldsymbol{q} = \begin{bmatrix} \frac{\sqrt{2\,(c_{\theta_1} + 1)}}{2} \\ 0 \\ 0 \\ -\frac{\sqrt{2}s_{\theta_1}}{2\sqrt{c_{\theta_1} + 1}} \end{bmatrix}, {}^{\boldsymbol{2}}_{\boldsymbol{1}}\boldsymbol{q} = \begin{bmatrix} \frac{\sqrt{s_{\theta_2} + 1}}{2} \\ \frac{\sqrt{s_{\theta_2} + 1}}{2} \\ \frac{c_{\theta_2}}{2\sqrt{s_{\theta_2} + 1}} \\ \frac{c_{\theta_2}}{2\sqrt{s_{\theta_2} + 1}} \end{bmatrix}, {}^{\boldsymbol{3}}_{\boldsymbol{2}}\boldsymbol{q} = \begin{bmatrix} \frac{\sqrt{c_{\theta_3} + 1}}{2} \\ \frac{\sqrt{c_{\theta_3} + 1}}{2} \\ -\frac{s_{\theta_3}}{2\sqrt{c_{\theta_3} + 1}} \\ -\frac{s_{\theta_3}}{2\sqrt{c_{\theta_3} + 1}} \end{bmatrix} \text{ and } {}^{\boldsymbol{4}}_{\boldsymbol{3}}\boldsymbol{q} = \begin{bmatrix} \frac{\sqrt{c_{\theta_4} + 1}}{2} \\ -\frac{\sqrt{c_{\theta_4} + 1}}{2} \\ \frac{s_{\theta_4}}{2\sqrt{c_{\theta_4} + 1}} \\ -\frac{s_{\theta_4}}{2\sqrt{c_{\theta_4} + 1}} \end{bmatrix}. \quad (11)$$

Finally, the equivalent quaternion form of Eq. (1) is:

$${}^{\boldsymbol{k}}\overline{\boldsymbol{\omega}}_{\boldsymbol{k}} = {}^{\boldsymbol{k}}_{\boldsymbol{k-1}}\boldsymbol{q} \otimes {}^{\boldsymbol{k-1}}\overline{\boldsymbol{\omega}}_{\boldsymbol{k-1}} \otimes {}^{\boldsymbol{k}}_{\boldsymbol{k-1}}\boldsymbol{q}^* + \begin{bmatrix} 0 & 0 & 0 & \dot{\theta}_k \end{bmatrix}, \quad (k = 1, 2, 3, 4), \quad (12)$$

which can be calculated iteratively since ${}^{\boldsymbol{0}}\boldsymbol{\omega_0} = \begin{bmatrix} 0 & 0 & 0 & 0 \end{bmatrix}^\intercal$ (the CMG fixed base position does not change in time).

The resulting four bodies angular velocity vectors in quaternion form are:

$${}^{\boldsymbol{1}}\overline{\boldsymbol{\omega}}_{\boldsymbol{1}} = \begin{bmatrix} 0 \\ 0 \\ 0 \\ \dot{\theta}_1 \end{bmatrix}, {}^{\boldsymbol{2}}\overline{\boldsymbol{\omega}}_{\boldsymbol{2}} = \begin{bmatrix} 0 \\ c_{\theta_2}\dot{\theta}_1 \\ -s_{\theta_2}\dot{\theta}_1 \\ \dot{\theta}_2 \end{bmatrix}, {}^{\boldsymbol{3}}\overline{\boldsymbol{\omega}}_{\boldsymbol{3}} = \begin{bmatrix} 0 \\ -s_{\theta_3}\dot{\theta}_2 + c_{\theta_3}c_{\theta_2}\dot{\theta}_1 \\ -c_{\theta_3}\dot{\theta}_2 - s_{\theta_3}c_{\theta_2}\dot{\theta}_1 \\ \dot{\theta}_3 - s_{\theta_2}\dot{\theta}_1 \end{bmatrix} \text{ and } {}^{\boldsymbol{4}}\overline{\boldsymbol{\omega}}_{\boldsymbol{4}} = \begin{bmatrix} 0 \\ s_{\theta_4}\dot{\theta}_3 - c_{\theta_4}s_{\theta_3}\dot{\theta}_2 + (c_{\theta_4}c_{\theta_3}c_{\theta_2} - s_{\theta_4}s_{\theta_2})\,\dot{\theta}_1 \\ c_{\theta_4}\dot{\theta}_3 + s_{\theta_4}s_{\theta_3}\dot{\theta}_2 - (s_{\theta_4}c_{\theta_3}c_{\theta_2} + c_{\theta_4}s_{\theta_2})\,\dot{\theta}_1 \\ \dot{\theta}_4 + c_{\theta_3}\dot{\theta}_2 + s_{\theta_3}c_{\theta_2}\dot{\theta}_1 \end{bmatrix}, \quad (13)$$

and the angular velocity vectors ${}^{\boldsymbol{k}}\boldsymbol{\omega_k}$, which will be used in the following dynamics stage of the modeling process, can be extracted withdrawing its scalar part since ${}^{\boldsymbol{k}}\overline{\boldsymbol{\omega}}_{\boldsymbol{k}} = \begin{bmatrix} 0 & {}^{\boldsymbol{k}}\boldsymbol{\omega_k} \end{bmatrix}^\intercal$.

2.3 Dynamics stage

For plant dynamics stage, the Gibbs-Appell equations are first considered (Baruh, 1999):

$$U_k = \sum_{i=1}^{N} \left(\frac{\partial \boldsymbol{v}_{\boldsymbol{G_i}}}{\partial u_k} \cdot \boldsymbol{F_i} + \frac{\partial \boldsymbol{\omega_i}}{\partial u_k} \cdot \boldsymbol{M}_{\boldsymbol{G_i}} \right), \quad (k = 1, \ldots, n), \quad (14)$$

in which i is related to Nth plant body and k is related to the nth degree of freedom (DOF); moreover, $\boldsymbol{F_i}$ and $\boldsymbol{M_{G_i}}$ denote the resultant vector of all forces external to the ith body and the resultant external moment vector about the center of mass of the ith body, $\boldsymbol{v_{G_i}}$ and $\boldsymbol{\omega_i}$ denote the velocity vector of center of mass and the angular velocity vector of the ith body, and u_k is the kth quasi-velocity.

This equation is recognized as the generalized force composed of two parts, the first one is the translational part and the second one is the rotational part. Thereby, it is considered the Kane's dynamical equations (Kane *et al.*, 1983):

$$U_k + \widetilde{U}_k = 0, \quad (k = 1, \ldots, n), \tag{15}$$

in which $\widetilde{U}_k$ is the generalized inertia force, defined as:

$$\widetilde{U}_k = \sum_{i=1}^{N} \left(\frac{\partial \boldsymbol{v_{G_i}}}{\partial u_k} \cdot \widetilde{\boldsymbol{F}}_{\boldsymbol{i}} + \frac{\partial \boldsymbol{\omega_i}}{\partial u_k} \cdot \widetilde{\boldsymbol{M}}_{\boldsymbol{G_i}} \right), \quad (k = 1, \ldots, n), \tag{16}$$

in which $\widetilde{\boldsymbol{F}}_{\boldsymbol{i}} = -m_i \boldsymbol{a_{G_i}}$ is the resultant inertia force vector acting through the center of mass of the ith body and $\widetilde{\boldsymbol{M}}_{\boldsymbol{G_i}} = -d\boldsymbol{H_{G_i}}/dt$ is the resultant inertia torque vector ($\boldsymbol{H_{G_i}}$ is the angular momentum about the center of mass of the ith body).

As the ECP CMG bodies do not have translational displacement, the first part of the sum in Eq. (14) and Eq. (16) vanish, and Eq. (15) results in the following equations of motion:

$$e_k = \sum_{i=1}^{N} \left(\frac{\partial \boldsymbol{\omega_i}}{\partial u_k} \cdot \boldsymbol{M_{G_i}} + \frac{\partial \boldsymbol{\omega_i}}{\partial u_k} \cdot \widetilde{\boldsymbol{M}}_{\boldsymbol{G_i}} \right) = 0, \quad (k = 1, \ldots, n), \tag{17}$$

in which $N = 4$ as CMG has four bodies ($i = 1, 2, 3, 4$ with $i = 1$ related to body A, $i = 2$ to body B, $i = 3$ to body C and $i = 4$ to body D), $n = 4$ as it has four DOF ($k = 1, 2, 3, 4$), $\boldsymbol{\omega_i} = {}^{\boldsymbol{i}}\boldsymbol{\omega_i}$ obtained in plant kinematics stage, defined in Eq. (13), and the quasi-velocities are defined as $u_k = \dot{\theta}_k$.

Solving Eq. (17) for $k = 1, 2, 3, 4$ and rewriting it in a matrix form:

$$\underbrace{\begin{bmatrix} e_1 \\ e_2 \\ e_3 \\ e_4 \end{bmatrix}}_{\boldsymbol{e}_{(4\times1)}} = \underbrace{\begin{bmatrix} \frac{\partial \boldsymbol{\omega_1}^\intercal}{\partial u_1} & \frac{\partial \boldsymbol{\omega_2}^\intercal}{\partial u_1} & \frac{\partial \boldsymbol{\omega_3}^\intercal}{\partial u_1} & \frac{\partial \boldsymbol{\omega_4}^\intercal}{\partial u_1} \\ \frac{\partial \boldsymbol{\omega_1}^\intercal}{\partial u_2} & \frac{\partial \boldsymbol{\omega_2}^\intercal}{\partial u_2} & \frac{\partial \boldsymbol{\omega_3}^\intercal}{\partial u_2} & \frac{\partial \boldsymbol{\omega_4}^\intercal}{\partial u_2} \\ \frac{\partial \boldsymbol{\omega_1}^\intercal}{\partial u_3} & \frac{\partial \boldsymbol{\omega_2}^\intercal}{\partial u_3} & \frac{\partial \boldsymbol{\omega_3}^\intercal}{\partial u_3} & \frac{\partial \boldsymbol{\omega_4}^\intercal}{\partial u_3} \\ \frac{\partial \boldsymbol{\omega_1}^\intercal}{\partial u_4} & \frac{\partial \boldsymbol{\omega_2}^\intercal}{\partial u_4} & \frac{\partial \boldsymbol{\omega_3}^\intercal}{\partial u_4} & \frac{\partial \boldsymbol{\omega_4}^\intercal}{\partial u_4} \end{bmatrix}}_{\boldsymbol{D}_{(4\times12)}} \underbrace{\begin{bmatrix} \boldsymbol{M_{G_1}} - \dot{\boldsymbol{H}}_{\boldsymbol{G_1}} \\ \boldsymbol{M_{G_2}} - \dot{\boldsymbol{H}}_{\boldsymbol{G_2}} \\ \boldsymbol{M_{G_3}} - \dot{\boldsymbol{H}}_{\boldsymbol{G_3}} \\ \boldsymbol{M_{G_4}} - \dot{\boldsymbol{H}}_{\boldsymbol{G_4}} \end{bmatrix}}_{\boldsymbol{f}_{(12\times1)}} = \underbrace{\begin{bmatrix} 0 \\ 0 \\ 0 \\ 0 \end{bmatrix}}_{\boldsymbol{0}_{4\times1}}, \tag{18}$$

where

$$\boldsymbol{D}_{(4\times12)} = \begin{bmatrix} 0 & 0 & 1 & c_{\theta_2} & -s_{\theta_2} & 0 & c_{\theta_2}c_{\theta_3} & -c_{\theta_2}s_{\theta_3} & -s_{\theta_2} & c_{\theta_2}c_{\theta_3}c_{\theta_4} - s_{\theta_2}s_{\theta_4} & -c_{\theta_2}c_{\theta_3}s_{\theta_4} - s_{\theta_2}c_{\theta_4} & c_{\theta_2}s_{\theta_3} \\ 0 & 0 & 0 & 0 & 0 & 1 & -s_{\theta_3} & -c_{\theta_3} & 0 & -c_{\theta_4}s_{\theta_3} & s_{\theta_3}s_{\theta_4} & c_{\theta_3} \\ 0 & 0 & 0 & 0 & 0 & 0 & 0 & 0 & 1 & s_{\theta_4} & c_{\theta_4} & 0 \\ 0 & 0 & 0 & 0 & 0 & 0 & 0 & 0 & 0 & 0 & 0 & 1 \end{bmatrix},$$

$$\boldsymbol{M_{G_1}} = \begin{bmatrix} 0 \\ 0 \\ -T_1 c_{\theta_2} s_{\theta_3} + T_2 s_{\theta_2} \end{bmatrix}, \; \boldsymbol{M_{G_2}} = \begin{bmatrix} 0 \\ 0 \\ -T_1 c_{\theta_3} \end{bmatrix}, \; \boldsymbol{M_{G_3}} = \begin{bmatrix} 0 \\ 0 \\ T_2 \end{bmatrix}, \; \boldsymbol{M_{G_4}} = \begin{bmatrix} 0 \\ 0 \\ T_1 \end{bmatrix},$$

$$\dot{\boldsymbol{H}}_{\boldsymbol{G_1}} = \begin{bmatrix} 0 \\ 0 \\ K_A \ddot{\theta}_1 \end{bmatrix}, \; \dot{\boldsymbol{H}}_{\boldsymbol{G_2}} = \begin{bmatrix} K_B c_{\theta_2} \ddot{\theta}_1 + (I_B - J_B - K_B)\, s_{\theta_2} \dot{\theta}_2 \dot{\theta}_1 \\ -I_B s_{\theta_2} \ddot{\theta}_1 - (I_B + J_B - K_B)\, c_{\theta_2} \dot{\theta}_2 \dot{\theta}_1 \\ J_B \ddot{\theta}_2 - (I_B - K_B)\, c_{\theta_2} s_{\theta_2} \dot{\theta}_1^2 \end{bmatrix},$$

$$\dot{\boldsymbol{H}}_{\boldsymbol{G_3}} = \begin{bmatrix} -K_C \left(s_{\theta_3} \ddot{\theta}_2 - c_{\theta_2} c_{\theta_3} \ddot{\theta}_1 + c_{\theta_3} \dot{\theta}_3 \dot{\theta}_2 + c_{\theta_2} s_{\theta_3} \dot{\theta}_3 \dot{\theta}_1 + s_{\theta_2} c_{\theta_3} \dot{\theta}_2 \dot{\theta}_1 \right) - (I_C - J_C) \left(\dot{\theta}_3 - s_{\theta_2} \dot{\theta}_1 \right) \left(c_{\theta_3} \dot{\theta}_2 + c_{\theta_2} s_{\theta_3} \dot{\theta}_1 \right) \\ -J_C \left(c_{\theta_3} \ddot{\theta}_2 + c_{\theta_2} s_{\theta_3} \ddot{\theta}_1 - s_{\theta_3} \dot{\theta}_3 \dot{\theta}_2 + c_{\theta_2} c_{\theta_3} \dot{\theta}_3 \dot{\theta}_1 - s_{\theta_2} s_{\theta_3} \dot{\theta}_2 \dot{\theta}_1 \right) + (I_C - K_C) \left(\dot{\theta}_3 - s_{\theta_2} \dot{\theta}_1 \right) \left(s_{\theta_3} \dot{\theta}_2 - c_{\theta_2} c_{\theta_3} \dot{\theta}_1 \right) \\ I_C \left(\ddot{\theta}_3 - s_{\theta_2} \ddot{\theta}_1 - c_{\theta_2} \dot{\theta}_2 \dot{\theta}_1 \right) + (J_C - K_C) \left(c_{\theta_3} \dot{\theta}_2 + c_{\theta_2} s_{\theta_3} \dot{\theta}_1 \right) \left(s_{\theta_3} \dot{\theta}_2 - c_{\theta_2} c_{\theta_3} \dot{\theta}_1 \right) \end{bmatrix},$$

$$\dot{\boldsymbol{H}}_{\boldsymbol{G_4}} = \begin{bmatrix} I_D \left[s_{\theta_4} \ddot{\theta}_3 - s_{\theta_3} c_{\theta_4} \ddot{\theta}_2 - \alpha \ddot{\theta}_1 + c_{\theta_4} \dot{\theta}_4 \dot{\theta}_3 + s_{\theta_3} s_{\theta_4} \dot{\theta}_4 \dot{\theta}_2 - \beta \dot{\theta}_4 \dot{\theta}_1 - c_{\theta_3} c_{\theta_4} \dot{\theta}_3 \dot{\theta}_2 - c_{\theta_2} s_{\theta_3} c_{\theta_4} \dot{\theta}_3 \dot{\theta}_1 - \gamma \dot{\theta}_2 \dot{\theta}_1 \right] - \epsilon \\ I_D \left[c_{\theta_4} \ddot{\theta}_3 + s_{\theta_3} s_{\theta_4} \ddot{\theta}_2 - \beta \ddot{\theta}_1 - s_{\theta_4} \dot{\theta}_4 \dot{\theta}_3 + s_{\theta_3} c_{\theta_4} \dot{\theta}_4 \dot{\theta}_2 + \alpha \dot{\theta}_4 \dot{\theta}_1 + c_{\theta_3} s_{\theta_4} \dot{\theta}_3 \dot{\theta}_2 + c_{\theta_2} s_{\theta_3} s_{\theta_4} \dot{\theta}_3 \dot{\theta}_1 - \delta \dot{\theta}_2 \dot{\theta}_1 \right] + \eta \\ J_D \left(\ddot{\theta}_4 + c_{\theta_3} \ddot{\theta}_2 + c_{\theta_2} s_{\theta_3} \ddot{\theta}_1 - s_{\theta_3} \dot{\theta}_3 \dot{\theta}_2 + c_{\theta_2} c_{\theta_3} \dot{\theta}_3 \dot{\theta}_1 - s_{\theta_2} s_{\theta_3} \dot{\theta}_2 \dot{\theta}_1 \right) \end{bmatrix},$$

$$\text{with } \alpha = \left(s_{\theta_2}s_{\theta_4} - c_{\theta_2}c_{\theta_3}c_{\theta_4}\right),\ \beta = \left(s_{\theta_2}c_{\theta_4} + c_{\theta_2}c_{\theta_3}s_{\theta_4}\right),\ \gamma = \left(c_{\theta_2}s_{\theta_4} + s_{\theta_2}c_{\theta_3}c_{\theta_4}\right),\ \delta = \left(c_{\theta_2}c_{\theta_4} - s_{\theta_2}c_{\theta_3}s_{\theta_4}\right),$$
$$\epsilon = \left(I_D - J_D\right)\left(\dot{\theta}_4 + c_{\theta_3}\dot{\theta}_2 + c_{\theta_2}s_{\theta_3}\dot{\theta}_1\right)\left[c_{\theta_4}\dot{\theta}_3 + s_{\theta_3}s_{\theta_4}\dot{\theta}_2 - \left(s_{\theta_2}c_{\theta_4} + c_{\theta_2}c_{\theta_3}s_{\theta_4}\right)\dot{\theta}_1\right] \text{ and}$$
$$\eta = \left(I_D - J_D\right)\left(\dot{\theta}_4 + c_{\theta_3}\dot{\theta}_2 + c_{\theta_2}s_{\theta_3}\dot{\theta}_1\right)\left[s_{\theta_4}\dot{\theta}_3 - s_{\theta_3}c_{\theta_4}\dot{\theta}_2 - \left(s_{\theta_2}s_{\theta_4} - c_{\theta_2}c_{\theta_3}c_{\theta_4}\right)\dot{\theta}_1\right], \tag{19}$$

results in four nonlinear equations e_k that describe the CMG motion in a simplified way (as some nonlinear phenomena were not considered, like the bearings friction of plant joints), which are composed of bodies scalar moments of inertia I_m, J_m and K_m ($m = A, B, C, D$). Its values are described in Tab. 1, which some of them (I_B, J_B, K_B, K_C, I_D and J_D) are given in plant manual (Parks, 1999), and others (K_A, I_C and J_C) are obtained through procedures describe in it.

Table 1: CMG scalar moments of inertia values (in kgm^2).

Symbol	K_A	I_B	J_B	K_B	I_C	J_C	K_C	I_D	J_D
Values	0.0698	0.0119	0.0178	0.0297	0.0124	0.0278	0.0188	0.0148	0.0273

Considering the CMG parameters values in Tab. 1, the Eq. (18) generate a plant nonlinear model:

$$\begin{aligned} e_1 = {} & -0.0273\sin\left(\theta_3\right)\cos\left(\theta_2\right)\ddot{\theta}_4 + 0.0272\sin\left(\theta_2\right)\ddot{\theta}_3 - 0.0215\cos\left(\theta_2\right)\cos\left(\theta_3\right)\sin\left(\theta_3\right)\ddot{\theta}_2 \ldots \\ & - \left[0.0215\sin^2\left(\theta_3\right)\cos^2\left(\theta_2\right) - 0.0242\sin^2\left(\theta_2\right) + 0.1331\right]\ddot{\theta}_1 - 0.0273\cos\left(\theta_3\right)\cos\left(\theta_2\right)\dot{\theta}_4\dot{\theta}_3 \ldots \\ & + 0.0273\sin\left(\theta_3\right)\sin\left(\theta_2\right)\dot{\theta}_4\dot{\theta}_2 + \left[0.0430\sin^2\left(\theta_3\right) + 0.0057\right]\cos\left(\theta_2\right)\dot{\theta}_3\dot{\theta}_2 \ldots \\ & - 0.0430\cos^2\left(\theta_2\right)\cos\left(\theta_3\right)\sin\left(\theta_3\right)\dot{\theta}_3\dot{\theta}_1 + 0.0215\sin\left(\theta_2\right)\cos\left(\theta_3\right)\sin\left(\theta_3\right)\dot{\theta}_2^2 \ldots \\ & + \left[0.0430\sin^2\left(\theta_3\right) + 0.0484\right]\cos\left(\theta_2\right)\sin\left(\theta_2\right)\dot{\theta}_2\dot{\theta}_1 = 0 \end{aligned} \tag{20}$$

$$\begin{aligned} e_2 = {} & -0.0273\cos\left(\theta_3\right)\ddot{\theta}_4 + \left[0.0215\sin^2\left(\theta_3\right) - 0.0729\right]\ddot{\theta}_2 - 0.0215\cos\left(\theta_2\right)\cos\left(\theta_3\right)\sin\left(\theta_3\right)\ddot{\theta}_1 \ldots \\ & + 0.0273\sin\left(\theta_3\right)\dot{\theta}_4\dot{\theta}_3 - 0.0273\sin\left(\theta_3\right)\sin\left(\theta_2\right)\dot{\theta}_4\dot{\theta}_1 + 0.0430\cos\left(\theta_3\right)\sin\left(\theta_3\right)\dot{\theta}_3\dot{\theta}_2 \ldots \\ & + \left[0.0430\sin^2\left(\theta_3\right) - 0.0487\right]\cos\left(\theta_2\right)\dot{\theta}_3\dot{\theta}_1 - \left[0.0215\sin^2\left(\theta_3\right) + 0.0242\right]\cos\left(\theta_2\right)\sin\left(\theta_2\right)\dot{\theta}_1^2 = 0 \end{aligned} \tag{21}$$

$$\begin{aligned} e_3 = {} & T_2 - 0.0272\ddot{\theta}_3 + 0.0272\sin\left(\theta_2\right)\ddot{\theta}_1 - 0.0273\sin\left(\theta_3\right)\dot{\theta}_4\dot{\theta}_2 + 0.0273\cos\left(\theta_3\right)\cos\left(\theta_2\right)\dot{\theta}_4\dot{\theta}_1 \ldots \\ & - 0.0215\cos\left(\theta_3\right)\sin\left(\theta_3\right)\dot{\theta}_2^2 - \left[0.0430\sin^2\left(\theta_3\right) - 0.0487\right]\cos\left(\theta_2\right)\dot{\theta}_2\dot{\theta}_1 \ldots \\ & + 0.0215\cos^2\left(\theta_2\right)\cos\left(\theta_3\right)\sin\left(\theta_3\right)\dot{\theta}_1^2 = 0 \end{aligned} \tag{22}$$

$$\begin{aligned} e_4 = {} & T_1 - 0.0273\Big[\ddot{\theta}_4 + \cos\left(\theta_3\right)\ddot{\theta}_2 + \sin\left(\theta_3\right)\cos\left(\theta_2\right)\ddot{\theta}_1 - \sin\left(\theta_3\right)\dot{\theta}_3\dot{\theta}_2 + \cos\left(\theta_3\right)\cos\left(\theta_2\right)\dot{\theta}_3\dot{\theta}_1 \ldots \\ & - \sin\left(\theta_3\right)\sin\left(\theta_2\right)\dot{\theta}_2\dot{\theta}_1\Big] = 0 \end{aligned} \tag{23}$$

As the CMG scalar moments of inertia values are imprecise, the generated plant nonlinear model [Eq. (20) to Eq. (23)] needs to be validated, in which numerical simulations of two tests are considered and described in the following section.

3. RESULTS AND DISCUSSION

Two tests are considered to analyze the plant main characteristics (precession and nutation) in order to validate the generated plant nonlinear model, which is used in numerical simulations. Its results are then compared with the ones obtained from practical experiments with the real plant.

Generically, the precession phenomenon is the orientation change of the rotation axis of a rotating body and the nutation phenomenon is the rotation axis vibration that occurs when a body is under precession action.

The Matlab/Simulink software is used for both numerical simulations and practical experiments, in which all initial conditions are considered null, i.e. $\theta_{k_0} = 0$ radians and $\dot{\theta}_{k_0} = 0$ radians per second, and bodies angular velocities $\dot{\theta}_k$ are indirectly obtained from backward Euler method with their respective angular positions θ_k, which are directly calculated in simulation cases and directly measured by CMG incremental encoders in experiment cases.

The first test analyzes the plant precession in order to calculate its rate, and the second test analyzes the plant nutation in order to calculate its frequency. Their procedures are detailed at Parks (1999) and summed up here.

Both tests procedures operate with axis #2 brake actuated and begin with the activation of a simple PI controller to elevate and keep the rotor velocity at $\dot{\theta}_4 = 41,8879$ radians per second and, at instant $t = 15$ seconds, a motor #2 torque (T_2) is applied.

In the first test (precession test), the applied motor #2 torque is $T_2 = 0.58$ Newton-metre (20% of its saturation value) for 8 seconds. Thus, the inner gimbal (body C) is dislocated from its initial position, changing the orientation of rotor rotation axis, which generates the gyroscopic torque. It in turn rotates the rotating base (body A) with a constant angular velocity $\dot{\theta}_1$ in steady state, which value is the plant precession rate.

And in the second test (nutation test), the applied motor #2 torque is $T_2 = 1.45$ Newton-metre (50% of its saturation value) for 0.05 seconds, i.e. an enough brief torque signal to excite the plant. Thus, the inner gimbal (body C) presents the reaction known as nutation, in which its angular velocity $\dot{\theta}_3$ oscillates with a certain frequency $f_{\text{nut}} = 2\pi/T_{\text{nut}}$ (the plant nutation frequency) in radians per second, which is calculated measuring its period T_{nut} in seconds.

The results obtained from numerical simulations with the generated nonlinear model and practical experiments with the real plant are presented below.

Figure 3 shows the simulation and experiment results obtained from the precession test, in which graphics from Fig. 3a (simulation) and Fig. 3b (experiment) illustrate bodies C and A angular velocities ($\dot{\theta}_3(t)$ and $\dot{\theta}_1(t)$). As the bearing frictions was not considered in the modeling process, $\dot{\theta}_3(t)$ and $\dot{\theta}_1(t)$ obtained from simulation (Fig. 3a) oscillate without loosing energy, as expected.

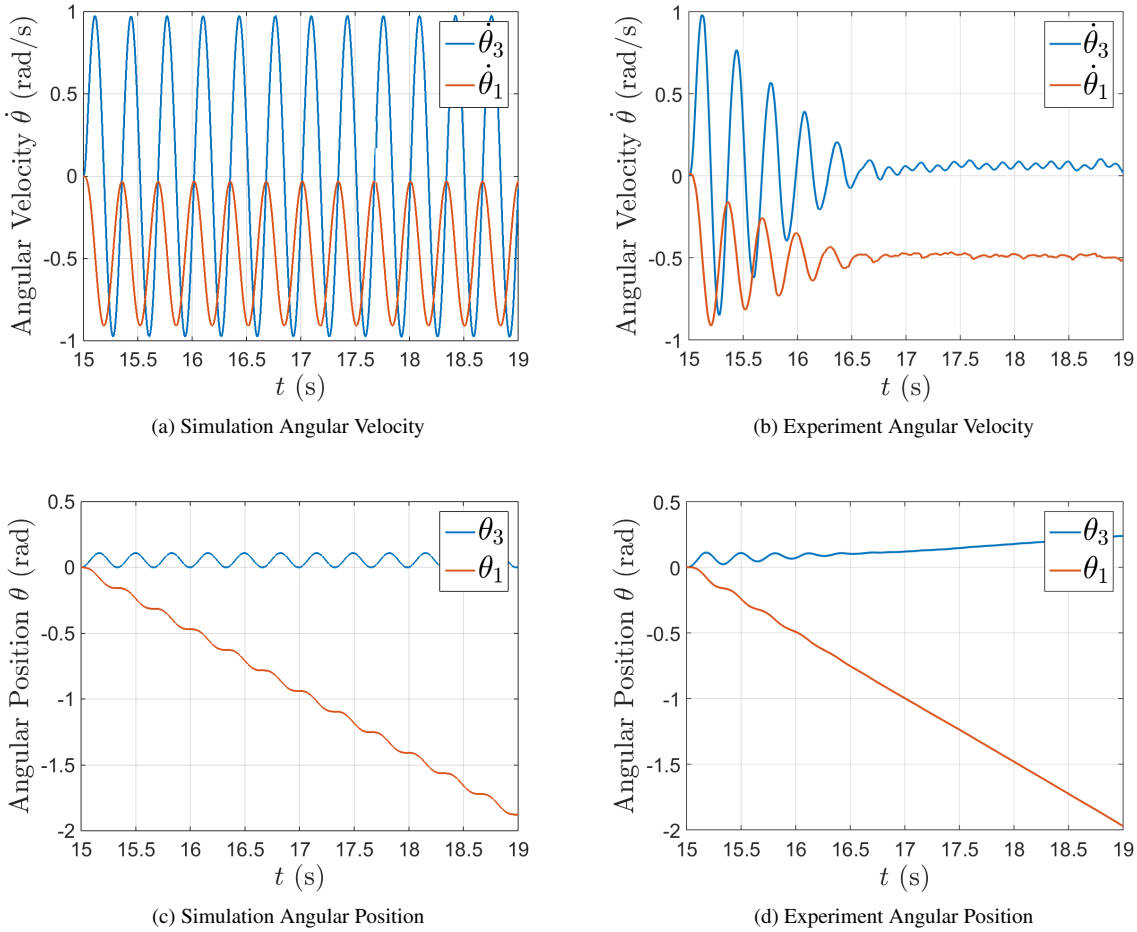

(a) Simulation Angular Velocity

(b) Experiment Angular Velocity

(c) Simulation Angular Position

(d) Experiment Angular Position

Figure 3: Precession test results.

Thus, its is opted to calculate the precession rate (constant value of $\dot{\theta}_1$ in steady state) from the difference of θ_1 values collected at instants $t_i = 17$ seconds and $t_f = 18$ seconds from graphics of bodies C and A angular positions (θ_3 and θ_1) in Fig. 3c (simulation) and Fig. 3d (experiment). These values are described in Tab. 2.

The resulting simulation and experiment precession rates are $\dot{\theta}_{1_{\text{sim}}} = -0.4691$ rad/s and $\dot{\theta}_{1_{\text{exp}}} = -0.4834$ rad/s, respectively, leading to a model relative error $E_p\%$:

$$E_p\% = \left| \frac{\dot{\theta}_{1_{\text{sim}}} - \dot{\theta}_{1_{\text{exp}}}}{\dot{\theta}_{1_{\text{exp}}}} \right| \cdot 100\% = \left| \frac{-0.4691 + 0.4834}{-0.4834} \right| \cdot 100\% = 2.96\%. \tag{24}$$

Table 2: Collected values from precession test.

θ_1	$t_i = 17$s	$t_f = 18$s	Precession Rate $\left[\dot{\theta}_1 = (\theta_{1_{t_f}} - \theta_{1_{t_i}})/1\right]$
Simulation	-0.9384 rad	-1.4075 rad	-0.4691 rad/s
Experiment	-0.9972 rad	-1.4806 rad	-0.4834 rad/s

Figure 4 shows the simulation and experiment results obtained from the nutation test, in which graphics from Fig. 4a (simulation) and Fig. 4b (experiment) illustrate bodies C and A angular velocities ($\dot{\theta}_3(t)$ and $\dot{\theta}_1(t)$).

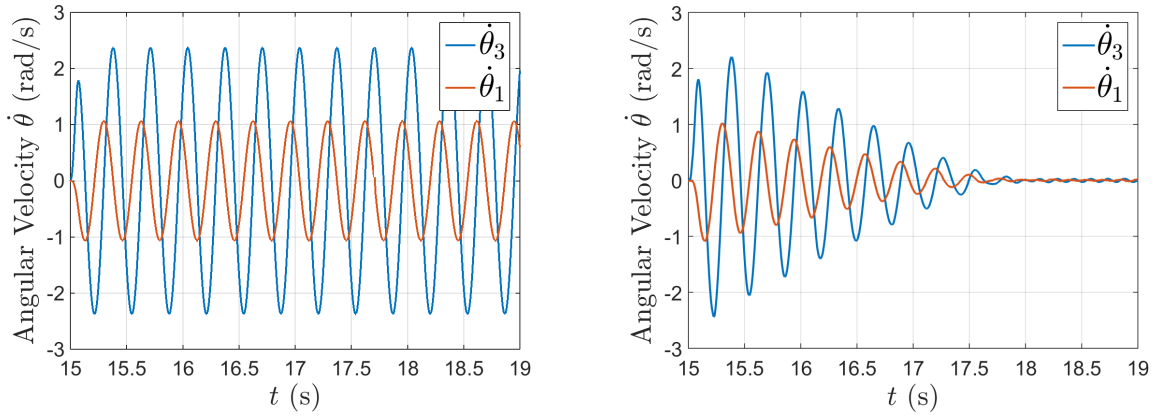

(a) Simulation Angular Velocity

(b) Experiment Angular Velocity

Figure 4: Nutation test results.

It is opted to collect three complete periods of $\dot{\theta}_3$ oscillation in steady state, in order to calculate the average nutation frequency. Thereby, the instant time values of the beginning of second period cycle (t_i) and the ending of fourth period cycle (t_f) are collected and described in Tab. 3.

Table 3: Collected values from nutation test.

$\dot{\theta}_3$	t_i (2nd cycle beginning)	t_f (4th cycle ending)	Average Nutation Period $[T_{\text{nut}} = (t_f - t_i)/3]$
Simulation	15.30s	16.30s	0.3333s
Experiment	15.30s	16.26s	0.3200s

The resulting simulation and experiment average nutation frequencies are $f_{\text{nut}_{\text{sim}}} = 2\pi/0.3333 = 18.8496$ rad/s and $f_{\text{nut}_{\text{exp}}} = 2\pi/0.3200 = 19.6350$ rad/s, respectively, leading to a model relative error $E_n\%$:

$$E_n\% = \left|\frac{f_{\text{nut}_{\text{sim}}} - f_{\text{nut}_{\text{exp}}}}{f_{\text{nut}_{\text{exp}}}}\right| \cdot 100\% = \left|\frac{18.8496 - 19.6350}{19.6350}\right| \cdot 100\% = 4.00\% \tag{25}$$

Highlighting again, as bearings friction were not considered in the modeling process, the simulation results obtained from both tests (Fig. 3a, Fig. 3c and Fig. 4a) have an oscillatory characteristic due to absence of energy loss, as expected, which do not discountenance the plant main characteristics.

4. CONCLUSIONS

Regardless of the imprecision of CMG scalar moments of inertia values and the fact that some nonlinear phenomena were not considered in the modeling process, as the bearings friction of plant joints, the plant main characteristics of the obtained nonlinear model were very close to the real ones as its relative errors were small, concluding that it is relatively satisfactory and suitable to be used for controllers design.

5. ACKNOWLEDGEMENTS

Authors thank Fundação de Amparo à Pesquisa do Estado de São Paulo (FAPESP) for grant 2013/25605-2.

6. REFERENCES

Abbas, H.S., Ali, A., Hashemi, S.M. and Werner, H., 2013. "LPV gain-scheduled control of a control moment gyroscope". In *American Control Conf. (ACC)*. pp. 6841–6846.

Abbas, H.S., Ali, A., Hashemi, S.M. and Werner, H., 2014. "LPV state-feedback control of a control moment gyroscope". *Control Engineering Practice*, Vol. 24, pp. 129–137.

Baruh, H., 1999. *Analytical dynamics*. WCB/McGraw-Hill Boston.

Bhat, S. and Tiwari, P.K., 2009. "Controllability of spacecraft attitude using control moment gyroscopes". *IEEE Trans. Autom. Control*, Vol. 54, No. 3, pp. 585–590.

Craig, J.J., 1989. *Introduction to Robotics: Mechanics and Control*, Vol. 2. Addison-Weslg.

Dam, E.B., Koch, M. and Lillholm, M., 1998. *Quaternions, interpolation and animation*, Vol. 2. Datalogisk Institut, Københavns Universitet.

Durand, S., Boisseau, B., Martinez-Molina, J.J., Marchand, N. and Raharijaona, T., 2014. "Event-based LQR with integral action". In *IEEE Emerging Technology and Factory Automation (ETFA)*. pp. 1–7.

ECP, 1990. "Model 750: Control Moment Gyroscope". Educational Control Products. 10 Mar. 2017 <http://www.ecpsystems.com/controls_ctrlgyro.htm>.

Funda, J., Taylor, R.H. and Paul, R.P., 1990. "On homogeneous transforms, quaternions, and computational efficiency". *IEEE Transactions on Robotics and Automation*, Vol. 6, No. 3, pp. 382–388.

Gagne, J., Piccin, O., Laroche, E., Diana, M. and Gangloff, J., 2012. "Gyrolock: Stabilizing the heart with control moment gyroscope (CMG); from concept to first in vivo assessments". *IEEE Trans. Robot. Autom.*, Vol. 28, No. 4, pp. 942–954.

Jazar, R.N., 2010. *Theory of applied robotics: kinematics, dynamics, and control*. Springer Science & Business Media.

Kane, T.R., Likins, P.W. and Levinson, D.A., 1983. *Spacecraft dynamics*.

Kuipers, J.B., 1999. *Quaternions and rotation sequences*. Princeton university press Princeton.

Mardan, M.F., Malik, M.B., Iqbal, S. and Ali, R., 2015. "Robust controller design for attitude control of control moment gyroscope". In *12th Int. Bhurban Conf. Appl. Sciences and Technology (IBCAST)*. pp. 163–168.

Parks, T.R., 1999. *Manual For Model 750 Control Moment Gyroscope*. ECP, Educational Control Products.

Spring, K.W., 1986. "Euler parameters and the use of quaternion algebra in the manipulation of finite rotations: A review". *Mechanism and Machine Theory*, Vol. 21, No. 5, pp. 365 – 373.

Yavuzoglu, E., Topal, E., Kutlu, A., Urek, H., Gulluoglu, M.E., Tarakcioglu, O., Yurtoglu, E., Akin, D., Celik, K., Ozyurt, C., Aydin, K. and Yilmaz, K., 2011. "Verification of control moment gyroscopes based attitude control systems for agile satellite missions". In *5th Int. Conf. Recent Advances in Space Technologies (RAST)*. pp. 547–553.

Yetkin, H., Kalouche, S., Vernier, M., Colvin, G., Redmill, K. and Ozguner, U., 2014. "Gyroscopic stabilization of an unmanned bicycle". In *American Control Conf. (ACC)*. pp. 4549–4554.

7. RESPONSIBILITY NOTICE

The authors are the only responsible for the printed material included in this paper.